International Journal of Computational and Experimental Science and ENgineering (IJCESEN)

Vol. 9-No.4 (2023) pp. 346-353
http://dergipark.org.tr/en/pub/ijcesen

Copyright © IJCESEN

ISSN: 2149-9144

Research Article

The Characterization of Welded AA 5005 Alloy with AA 5356 Filler Metals According to Slow Welding Rate Using by MIG Welding Technique

Günhan BAYRAK[1], Hüseyin MÜŞTAK[2*]

[1]Sakarya University of Applied Science, Arifiye Vocational School, 54580, Sakarya-Türkiye,
Email: gunhanb@subu.edu.tr - **ORCID:** 0000-0002-3837-0459

[2]ASAŞ Aluminyum Tic. A.Ş, 54400, Sakarya-Türkiye
Corresponding Email : huseyin.mustak@asastr.com - **ORCID:** 0000-0002-5109-2684

Article Info:

DOI: 10.22399/ijcesen.1357384
Received : 08 September 2023
Accepted : 08 November 2023

Keywords :

AA 5005 Alloy
MIG Weld
Welding Rate
NDT
Characterization

Abstract:

In the present study, AA 5005 cold rolled plate was used for welding application with AA 5356 filler materials using MIG welding process. Slow (780 mm/min) welding rate was applied for weld joint of the plate. After the welding operation, NDT tests (Visual Test, Liquid Penetrant Test, Radiography Test) and X ray Diffraction analyzes were applied to the welded plates for proving the weld quality and determination of the phases in the weld beat during the solidification of the weld pool. Then, microstructural color metallography technique was used for the investigations of grain size distribution of the weld joint and heat affected zone and base metal. Vickers microhardness tests applied on the cross-section of the weld joint together with HAZ and base metal. In addition these, tensile tests were realized for the determination of the mechanical properties of the welded cold worked AA 5005 alloy with AA5356.

1. Introduction

Aluminium AA 5005 alloy is a versatile and widely used aluminium-magnesium alloy known for its excellent corrosion resistance and formability. It belongs to the AA 5xxx series of aluminium alloys, which are non-precipitation hardenable and characterized by their high strength-to-weight ratio [1]. The presence of magnesium as the primary alloying element enhances the alloy's strength and weldability. Aluminium AA 5005 finds extensive application in various industries, including automotive, marine, and architectural sectors, where its corrosion resistance makes it ideal for outdoor and marine environments. This is why these alloys are called as marine alloys at the same time. Additionally, the alloy is favoured for its ease of fabrication, making it a popular choice for a wide range of structural and decorative applications [1,2].
MIG welding, also known as Gas Metal Arc Welding (GMAW), is a widely used and preferred welding process for Aluminium alloys because of its efficiency and versatility. MIG welding of aluminium alloys realized by a consumable electrode wire made of Aluminium or Aluminium alloys. The welding arc is formed between the electrode and the work-piece, with an externally supplied shielding gas, typically argon or a mixture of argon and helium, protecting the molten pool from atmospheric contamination [3]. MIG welding of Aluminium offers several advantages, including high welding speeds, good weld quality, and minimal post-weld clean up [4]. However, Aluminium's high thermal conductivity requires precise control of welding parameters to achieve proper fusion and prevent potential defects like porosity. With proper technique and parameter adjustment, MIG welding is an effective method for joining Aluminium components across a wide range of industries [3,5].
Welding rate in MIG welding for Aluminium alloys is a critical parameter that can significantly impact the welding process and the quality of the resulting welds. Welding rates, generally defined as travel speeds of the welding torch, can offer several advantages and challenges when working with Aluminium alloys [6,7]. Aluminium alloys have a relatively high thermal conductivity, meaning they dissipate heat quickly. By reducing the welding speed, welders can focus more heat on the joint, allowing for better penetration and fusion of the metal which will avoid lack of fusion. This can result

in stronger and more reliable welds, particularly in thicker sections or when welding dissimilar Aluminium alloys [5,8]. Slow rated welding also comes with potential risks that welders must be mindful of. One significant risk is the potential for excessive heat input and prolonged exposure to the weld pool. Slow welding rates can lead to higher heat concentration, causing the Aluminium to become more susceptible to distortion, warping, and burn-through and porosity. Welders must carefully manage the travel speed and adjust other welding parameters to avoid these issues and maintain optimal heat control [9,11].

The other side effect of slow welding speed can be undercut defect. Undercut is a common welding defect where the weld metal does not completely fill the joint, resulting in a groove or depression along the weld joint's edges. One of the factors that can contribute to the occurrence of undercut is the welding speed. Slow welding speeds can cause undercut faults due to the prolonged exposure of the weld metal to excessive heat. When the welding speed is slow, the heat input becomes higher, and the weld pool remains in a molten state for an extended period. The prolonged molten state of the weld pool can lead to excessive melting of the base metal at the edges of the joint. As a result, the molten metal flows away from the edges, causing a groove or depression, which is the undercut [10,11]. In the literature, it is observed that AA 4346 additive material is often preferred when welding AA 5005 alloys [12], however the mechanical properties of which is lower than that of the weld joint of the alloys with AA 5356 filler material.

The main goal of this study was to investigate the weldability, hardness and tensile properties and microstructural investigations of weld joints of marine AA 5005 alloy at low welding speed by using AA 5356 filler material.

2. Material and Methods

2.1 Preparing the samples and welding

AA 5005 aluminum alloy plates which are used in this study of which chemical composition and mechanical properties are shown in Table 1 and Table 2, respectively.

Table 1. *Chemical composition of AA 5005 alloy*

Si [%]	Fe [%]	Cu [%]	Mn [%]	Mg [%]	Zn [%]	Ti [%]	Cr [%]
0,1490	0,4042	0,0078	0,0299	0,5136	0,0067	-	0,0021

Table 2. *Mechanical properties of AA 5005 alloy plate*

Sample Direction °	Yield strength %0,2, MPa	Tensile strength, MPa	Elongation A_{50}, %
90	160	174	9
90	160	173	8,3
0	147	165	7,6
0	147	166	8,5

MIG welding was employed as the welding process, and Safra brand AA 5356 filler wire was utilized for the welding operation. Chemical composition and mechanical properties of filler wire are shown in Table 3 and Table 4, respectively.

Table 3. *Chemical composition of filler wire*

Si [%]	Fe [%]	Cu [%]	Mn [%]	Mg [%]	Zn [%]	Ti [%]	Cr [%]
0,25	0,40	0,10	0,05-0,2	4,5-5,5	0,10	0,15	0,1-0,3

Table 4. *Mechanical properties of filler wire*

ER5356 Mechanical Properties	
Yield Strength, MPa	>110
Elongation, %	17
Tensile Strength, MPa	240

The size of the starting test plate was 300 mm x 150 mm x 3mm. Before commencing the welding, meticulous cleaning of all plates was conducted with acetone to ensure a pristine surface free from contaminants. The prepared plates were then securely positioned and clamped in a welding fixture to ensure stable welding conditions. Fronius Transpuls Synergic 4000 robotic MIG welding machine was used for the precise and consistent welds, at pulse synergie mode. The welding process was carried out at a deliberately slow rate of 780 mm/min to explore its effects on the resulting weld joint and properties.

2.2 Non-Destructive tests

Visual control of weld seams is a critical aspect of the welding process, and it is conducted in accordance with the guidelines outlined in the EN ISO 13018 standard. This inspection method involves carefully examining the weld beat and

surrounding areas to detect any surface defects, discontinuities, or irregularities that could potentially compromise the integrity of the weld joint. Control criteria can be seen in Figure 1. Before control, weld beat was cleaned with a wire brush after then, the visual control of the weld beat was performed under 160 lux lighting conditions.

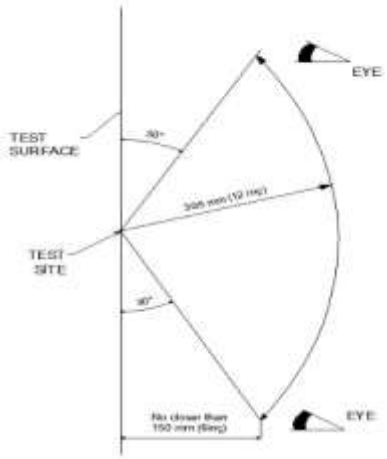

Figure 1. *TS EN ISO 10042 control criteria*

The penetrant test for welding seams was performed. The liquid penetrant method was utilized, and a penetrant liquid was applied to the surface of the weld seam and allowed to dwell for the specified time. The excess penetrant was then removed, and a developer was applied to draw out any indications of surface-breaking defects. The developer rendered the indications visible, and the weld seams were carefully examined for any potential cracks, porosity, or lack of fusion. The penetrant test proved to be an effective non-destructive testing method in detecting surface discontinuities, ensuring the quality and integrity of the welded components and structures.

Radiographic inspection is shown as the most important inspection method used to test the quality and reliability of welded joints among non-destructive testing methods. Therefore, in our study, radiographic examination was performed to detect potential internal defects or discontinuities in the weld seams. As part of this test, weld seams were exposed to X-rays by an ICM X-ray device with specific parameters as 150 kV tube voltages, 5 mA tube current. Then, X-ray films were taken and the weld seam area was carefully examined.

The weld zone was characterized by XRD analysis (Rigaku D/Max which has a wavelength of 1.54056 Å with a Cu Kα radiation.

2.3 Destructive tests

After grinding the weld seam, a tensile strength test was carried out for the welded parts. Welded parts are meticulously prepared in accordance with ASTM E-8 standard and ground to ensure homogeneity. The samples obtained in this way were subjected to tensile strength test using Zwick Roell Z050 Tensile Test Machine (Figure 2). The test speed was 10 mm/min and the load was 50 kgf. By recording the data obtained during the experiment, it was checked whether the welded joint is within the range of tensile strength values recommended in the literature.

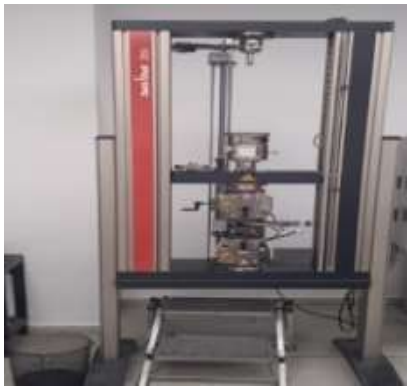

Figure 2*: Zwick Roell Z050 Tensile Test Machine*

Tensile test specimen dimensions is shown on the Figure 3.

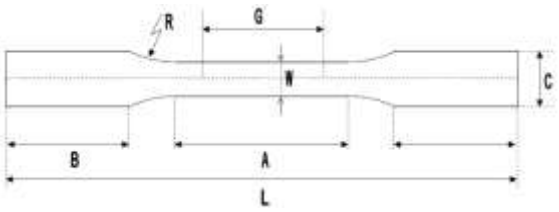

STANDART	STANDART
G = 50,00 ± 0,10 mm	A = 57 mm (min.)
W = 12,50 ± 0,05 mm	B = 50 mm
R = 12,5 mm (min.)	C = 20 mm
L = 200 mm (min.)	

Figure 3*: Tensile test specimen and its dimensions*

by going through cutting, grinding and polishing stages, and then their microstructures were examined

using by optical microscope and electron microscopy.

The macro test provides valuable information about the size, shape and general characteristics of the weld, helping to identify visible defects or irregularities. The macro testing using the NIKON SM2 allowed the samples to be examined on a larger scale to evaluate their overall appearance and macro structure.

After welding AA 5005 alloy with AA 5356 additional wire, microstructure examination tests of weld zone, HAZ and base metal were performed using NIKON Eclipse MA200 microscope. This test method provides valuable information about grain structure, phase distribution, and possible defects or irregularities present in welds.

Grain size analysis was carried out using Zeiss Scope A1 and grain sizes were measured by the intersection method. The samples were carefully observed and analysed with a Zeiss Scope A1 microscope and detailed examination of the grain structure was provided. Quantitative data on average grain sizes in the material were obtained by using the intersection method to measure grain sizes. This non-destructive testing approach helps to comprehensively evaluate the grain size distribution and its effect on the mechanical properties of the material.

The samples were examined using the ZEISS EVO MA15 scanning electron microscope. Changes in the microstructure and phase size distributions of the source transition zone were studied in the BSE image material contrast mode.

Hardness measurements were carried out on the samples using the Zwick Roell ZHV 10 microhardness tester, in which sequential measurements were taken at 500 micron intervals starting from the base metal, according to the ASTM- E92 standard. In these measurements, applied loads and dwell times are 10 grf and of 15s, respectively. In this way, a Microhardness Contour diagram was obtained using by Minitab 19 software.

3. Results and Discussions

The visual test results of the weld bead were examined and it was found that it complies with the TS EN ISO 10042 B criteria. During visual inspection, the weld bead and surrounding areas are carefully inspected for visible defects, discontinuities or irregularities. Inspection revealed that the weld piece displayed a satisfactory appearance with no signs of significant defects that could compromise its quality or structural integrity. The weld joint was observed to be well formed and free of any visible cracks, lack of melting or porosity.

The penetration test results of the weld bead were examined; < 3 mm surface porosity has been seen on the bead. This porosity had been occurred due to slow welding speed [9]. Porosity can be seen at Figure 4. But according to the TS EN ISO 23277 Level II standard, this scaled porosity is allowed. The penetration test involved inspecting the weld bead for any indications of incomplete fusion or penetration. The examination revealed that the weld bead exhibited satisfactory fusion and penetration, meeting the requirements specified in the TS EN ISO 23277 Level II standard. There were no indications of incomplete fusion or lack of penetration, indicating that the welding process was performed effectively, and the weld joint had achieved the desired level of fusion and penetration.

Figure 4: *Penetration Test*

In the radiography test conducted in this study, porosities were identified, similar to the observations in the penetration test. Similar to the findings of Zhan et al., it was observed that low welding speeds can lead to porosity formation. Some porosity formation was also observed at 780 mm/min welding speed. [15]. X-ray can be seen at Figure 5.

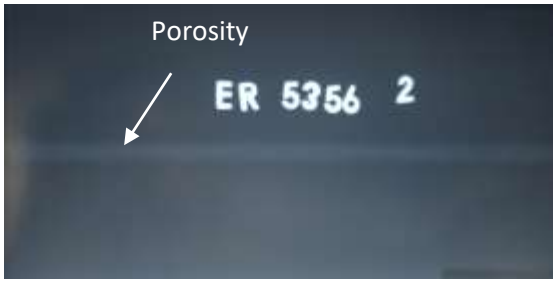

Figure 5: *X-Ray of weld seam*

The tensile test results, in accordance with TS EN ISO 15614-2 standard, met the condition of equal to or above "0" (Original condition; H_0) for the tensile strength. During the test, the test part was broken apart from the heat-affected zone (HAZ) (Figure 6). The yield strength was measured at 88 MPa, and the tensile strength recorded at 110 MPa (Table 5), the tensile strength minimum requirement of "0" condition tensile strength, which is set at 100 MPa. The successful outcome of the tensile test demonstrates the weld joint's excellent mechanical properties, as it withstood the applied tensile forces well above the minimum threshold. These results affirm the weld's reliability and structural integrity, meeting the stringent criteria outlined by the TS EN ISO 15614-2 standard.

Figure 6*: Sample after tensile test.*

Table 5: *Mechanical properties after welding*

Tensile Strength (MPa)	Yield Strength (MPa)
110	88

The macro test image (Figure 7) revealed the formation of a weld bead with a width of 4.90 mm and a depth of 3.44 mm. The height of the weld bead was measured to be 1.83 mm. These measurements indicate the dimensions and overall appearance of the weld bead on a larger scale.

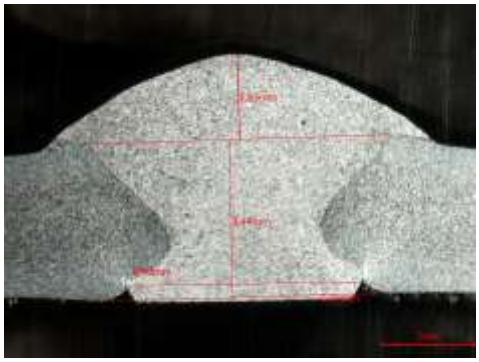

Figure 7: *Macro image of welding*

The micro test results revealed significant findings along the transition from fiber grains to recrystallization and regrowth grains. The examination displayed distinct microstructural changes, illustrating the transformation from initial fiber-like grains to newly recrystallized grains (Figure 8). Additionally, the presence of regrowth grains was evident, indicating the material's response to the welding thermal influence during welding. The differentiation of grain types from the base metal to the HAZ and fusion zone has significant implications for the mechanical properties and overall performance of the weld joint. The finer grain structure in the HAZ can lead to enhanced mechanical strength and improved resistance to certain forms of corrosion. On the other hand, the coarser grain structure in the fusion zone may result in reduced mechanical properties, such as lower tensile strength and increased susceptibility to brittle [13].

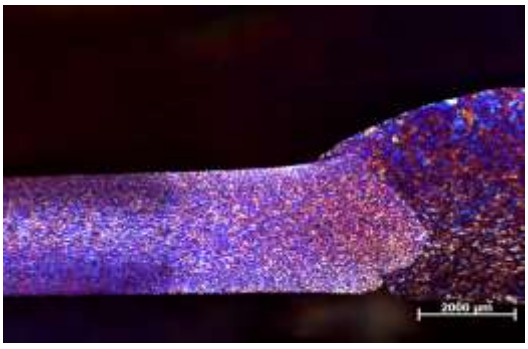

Figure 8: *Transition of grains*

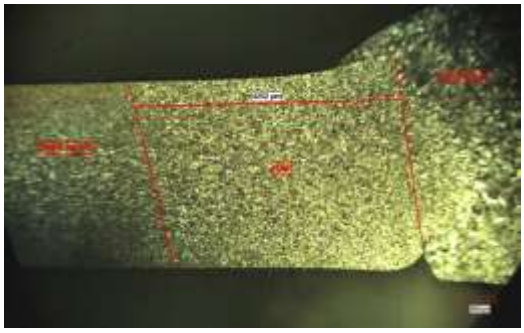

Figure 9: *HAZ measurement*

HAZ length was measured as 4252 microns (Figure 9).Grain size measurement using the intercept method revealed distinct differences between the heat-affected zone (HAZ) and the fusion zone. The HAZ exhibited an average grain size of 33.99 µm, indicating a finer microstructure compared to the fusion zone. In contrast, the fusion zone displayed a larger average grain size of 68.94 µm (Figure 10 and 11), suggesting coarser grains within this region.

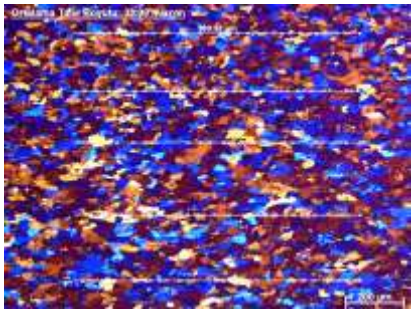

Figure 10: *HAZ grain size measurement*

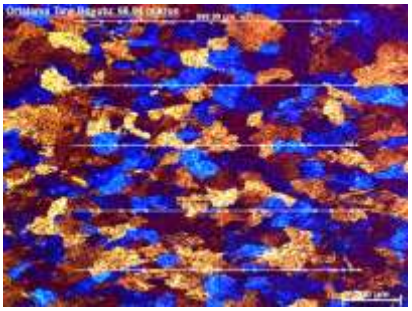

Figure 11: *Fusion zone grain size measurement*

The SEM analysis revealed the presence of small and numerous white contrasted particles in the microstructure. Additionally, black contrasted areas were observed, indicating the formation of porous regions in the weld metal. The effect of heat input during the welding process resulted in the occurrence of coarse and large-sized intermetallic phases within the welding zone. These findings provide valuable insights into the microstructural characteristics of the weld, shedding light on the distribution of particles and porosity, as well as the impact of heat on the formation of intermetallic phases. During the welding process, hydrogen can be introduced into the molten weld pool from various sources, such as moisture, contaminants, or the electrode coating. As the weld solidifies, the hydrogen can become trapped within the metal structure, forming hydrogen gas bubbles. These gas bubbles are responsible for the observed black contrast in the micrographs. The slow welding speed plays a crucial role in the hydrogen entrapment phenomenon. When the welding speed is slow, the solidification of the weld metal occurs at a slower rate. This extended solidification time provides more opportunities for the hydrogen atoms to diffuse and become trapped within the microstructure, leading to the formation of the black contrasted particles [14]. SEM image can be seen at Figure 12. Especially white parts took place grain boundaries and, in the grains are intermetallic phase (Al_3Mg_2) together with α-matrix phase (constituent gray parts). M.Bilgin et.al explained that the Al-Mg alloys includes Al_3Mg_2 and $Al_{12}Mg_{17}$ intermetallic phases in the welding zone and matrix (Figure 13) [16].

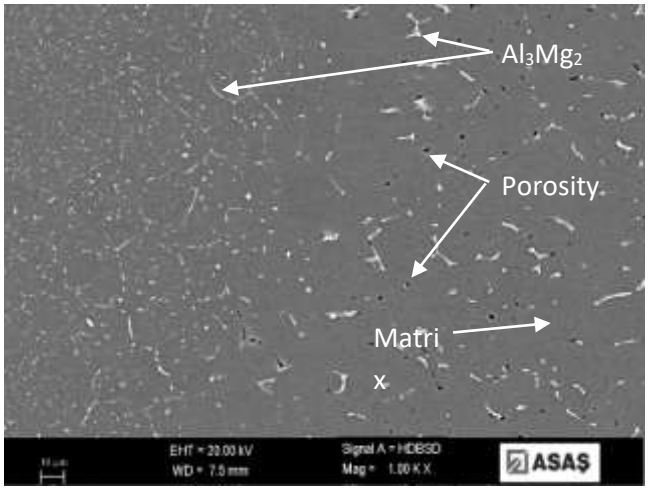

Figure 12: *SEM image at BSE mode*

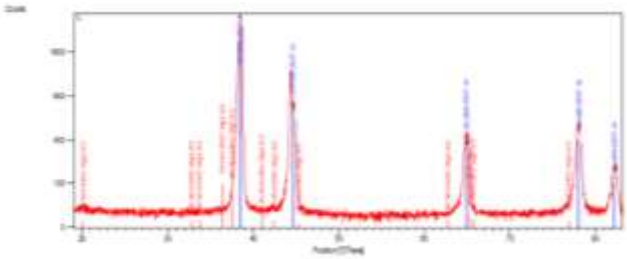

Figure 13:. *XRD analysis of the weld zone*

The hardness test results showed findings as the measurements transitioned from the base metal to the recrystallized heat-affected zone (HAZ) region. During this transition, the hardness values were observed to decrease. Although, in the weld bead characterized by grain growth, a notable increase in hardness up to 100 HV was observed, because of the including higher alloying elements including filler materials composition. These results highlight the significant influence of microstructural changes on the material's hardness properties within different regions of the weld joint. Microhardness Contour Graphic can be seen at Figure 14.

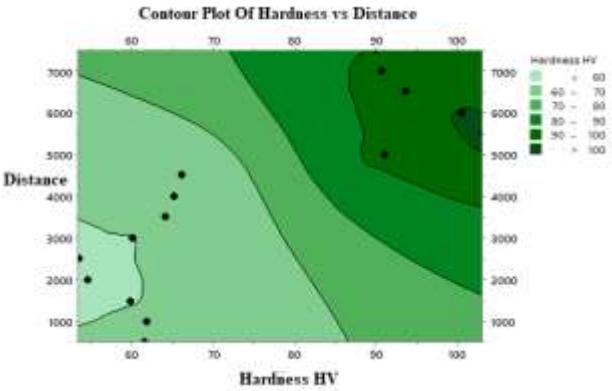

Figure 14: *Microhardness Contour diagram*

4. Conclusion

Based on the experimental results ;

1. The welding conducted at 780 mm/min welding speed was deemed suitable in terms of mechanical properties. However, during the radiographic and metallographic examinations, certain drawbacks were observed due to the low welding speed, resulting in high heat input. Grain size of heat-affected zone (HAZ) and the fusion zone are 33.99 µm and 68.94 µm, respectively.
2. AA 5005 alloy welded with AA 5356 exhibits that yield strength and tensile strength were 88 MPa and 110 MPa, respectively.
3. In comparison to the HAZ region, the weld bead contained significantly larger grains, with evident grain coarsening within the welding. The hardness was observed to decrease as it transitioned from the base metal to the HAZ region, while an increase in hardness was observed during the transition from the HAZ region to the weld bead. This can be attributed to the superior mechanical properties of the used 5356 filler wire compared to the 5005 alloy.

Overall, these findings provide valuable insights into the microstructural changes and mechanical properties of the welded joints, contributing to a comprehensive understanding of the welding process and the implications on the weld's performance and quality.

Author Statements:

- **Ethical approval:** The conducted research is not related to either human or animal use.
- **Conflict of interest:** The authors declare that they have no known competing financial interests or personal relationships that could have appeared to influence the work reported in this paper

- **Acknowledgement:** The authors declare that they have nobody or no-company to acknowledge.

- **Author contributions:** The authors declare that they have equal right on this paper.

- **Funding information:** The authors declare that there is no funding to be acknowledged.

- **Data availability statement:** The data that support the findings of this study are available on request from the corresponding author. The data are not publicly available due to privacy or ethical restrictions.

References

[1]Davis, J. R. (Ed.). (1999). Corrosion of aluminum and aluminum alloys. Asm International.

[2]. Quebbou, Z., Chafi, M., & Omari, L. E. H. (2021). Corrosion resistance of 5005 aluminum alloy by anodizing treatment in a mixture of phosphoric and boric acids. *Materials Today: Proceedings*, 37; 3854-3859.

[3]. Kaluç, E., & Taban, E. (2004). EN AW-5083-H321 Alüminyum alaşımının MIG, TIG ve sürtünen eleman ile birleştirme (FSW) kaynaklı bağlantılarının mekanik ve mikroyapısal özellikleri. *Mühendis ve Makina*, 46 (541); 40-51

[4]. Hooda, A., Dhingra, A., & Sharma, S. (2012). Optimization of MIG welding process parameters to predict maximum yield strength in AISI 1040. *International journal of Mechanical engineering and Robotics research*, 1(3); 203-213.

[5]Praveen, P., & Yarlagadda, P. K. D. V. (2005). Meeting challenges in welding of aluminum alloys through pulse gas metal arc welding. *Journal of Materials Processing Technology*, 164; 1106-1112.

[6]Mishra, B., Panda, R. R., & Mohanta, D. K. (2014). Metal Inert Gas (MIG) welding parameters optimization. *International Journal of Multidisciplinary and Current Research*, 2(1); 637-639.

[7] Olson, D. L., Dixon, R. D., & Liby, A. L. (Eds.). (2012). Welding: theory and practice. Elsevier.

[8] Wang, J., Feng, J. C., & Wang, Y. X. (2008). Microstructure of Al–Mg dissimilar weld made by cold metal transfer MIG welding. *Materials Science and Technology*, 24(7); 827-831.

[9] Çevik, B., & Koç, M. J. K. M. (2019). The effects of welding speed on the microstructure and mechanical properties of marine-grade aluminium (AA5754) alloy joined using MIG welding. *Metallic Materials/Kovové Materiály*, 57(5).

[10] Bhatt, D. A., & Mehta, H. R. (2015). Analyzing Effects of Weld Parameters for Increasing the Strength of Welded Joint on Mild Steel Material by Using the MIG Welding Process. Dimension, 300(300mm), 10mm.

[11] Himarosa, R. A., Rahman, M. B. N., Adi, R. K., Putra, L. A., & Nugroho, S. W. (2022). Effect of MIG Welding Speed Butt-Joint on Physical and Mechanical Properties of Materials AA 5083. *Materials Today: Proceedings*, 66, 3101-3106.

[12] EDITION, F. Arc Welding of Nonferrous Metals, Pg 16.

[13] Meseguer-Valdenebro, J. L., Martínez-Conesa, E., & Portoles, A. (2022). Influence of welding parameters on grain size, HAZ and degree of dilution of 6063-T5 alloy: optimization through the Taguchi method of the GMAW process. *The International Journal of Advanced Manufacturing Technology*, 120(9-10); 6515-6529.

[14] Atabaki, M. M., Yazdian, N., & Kovacevic, R. (2016). Partial penetration laser-based welding of aluminum alloy (AA 5083-H32). *Optik*, 127(16); 6782-6804.

[15] Zhan, X., Zhao, Y., Liu, Z., Gao, Q., & Bu, H. (2018). Microstructure and porosity characteristics of 5A06 aluminum alloy joints using laser-MIG hybrid welding. *Journal of Manufacturing Processes*, 35; 437-445.

[16] Bilgin, m., karabulut, ş., & özdemir, A. (2017). Alüminyum Magnezyum Alaşımlarının Sürtünme Karıştırma Kaynağı İle Kaynak Edilebilirliğinin Değerlendirilmesi. *Gazi University Journal of Science Part C: Design and Technology*, 5(2); 191-209.